Supplementary information for:

Deep magma degassing and volatile fluxes through volcanic hydrothermal systems: Insights from the Askja and Kverkfjöll volcanoes, Iceland

Eemu Ranta[1*], Sæmundur A. Halldórsson[1], Peter H. Barry[2], Shuhei Ono[3], Jóhann Gunnarsson Robin[1], Barbara I. Kleine[1,4], Andrea Ricci[5], Jens Fiebig[6], Árný E. Sveinbjörnsdóttir[1], Andri Stefánsson[1]

[1]*Nordic Volcanological Center, Institute of Earth Sciences, University of Iceland, Sturlugata 7, 102 Reykjavik, Iceland*
[2]*Marine Chemistry and Geochemistry Department, Woods Hole Oceanographic Institution, 266 Woods Hole Road, Woods Hole, MA 02543, USA*
[3]*Department of Earth, Atmospheric and Planetary Sciences, Massachusetts Institute of Technology, 77 Massachusetts Avenue, Cambridge, MA 02139, USA*
[4]*Now at GeoZentrum Nordbayern, Friedrich-Alexander-Universität Erlangen-Nuremberg, Schlossgarten 5, 91054 Erlangen, Germany*
[5]*Istituto Nazionale di Geofisica e Vulcanologia, Sezione di Palermo, Via Ugo La Malfa, 153, 90146 Palermo, Italy*
[6]*Institute of Geosciences, Goethe University, Altenhöferallee 1, 60438 Frankfurt/Main, Germany*

* corresponding author (eemu.ranta@helsinki.fi). Current address: Department of Geoscience and Geography, University of Helsinki, Gustaf Hällströmin katu 2, 00560 Helsinki, Finland.

Table of contents:

S1 Hydrogeology of Askja and Kverkfjöll

The steep topography of the Kverkfjöll central volcano results in a steeply dipping groundwater table, that flows out along numerous rivers on the flanks of the mountain massif. The Hveragil river flows out at ~1100 m, roughly at the estimated elevation of the initiation of boiling of the rising reservoir fluid (900-1200 m.a.s.l.). Mixing of the slightly boiled, or even unboiled reservoir water at ~300 °C and cold groundwater takes place at depth (Fig. 8), preventing further boiling upon ascent, making it a rare natural example of a diluted reservoir liquid. The mixing allows the Hveragil water to retain high dissolved CO_2 concentrations (c.f. Arnórsson and Barnes, 1983; Fig. S2a). Following boiling, the vapor phase rises above the ground water table to Hveradalur, which is dominated by acid-sulfate type geothermal activity and CO_2-H_2S rich fumarole discharge. Thus, the reservoir fluid is largely preserved in a diluted form in Hveragil, whereas only the gas phase is sampled at Hveradalur. Sampling the waters at Hveragil and the steam at Hveradalur can be seen a natural analogue to sampling of two-phase wells drilled into geothermal reservoirs.

In contrast to the steep groundwater table at Kverkfjöll, at Askja, the groundwater table is relatively flat, marked by the surface of Lake Öskjuvatn at 1050 m.a.s.l. Here, an upwelling, hot one-phase reservoir fluid boils at an estimated depth of ~300 m below the floor of Lake Öskjuvatn (Fig. 8). Above this depth, the vapor phase rises towards the surface along caldera faults and either escapes in fumaroles or condensates and dissolves into shallow groundwater. The boiled reservoir fraction may the dissipate laterally and mix with local groundwater before reaching the surface. The lack of upwellings of the boiled liquid phase may also indicate a younger age for the geothermal system at Askja (Heřmanská et al., 2019). No limiting condition at Askja, such as the topographic gradient in Kverkfjöll, blocks the backflow of steam-heated water to the aquifer to form a mixed local groundwater reservoir (Fig. 8). The generation of a mixed geothermal reservoir is also compounded by the lack of outflow for Lake Öskjuvatn. Hence, Lake Öskjuvatn and adjacent springs all seem to reflect various mixtures of non-thermal water, condensed steam and boiled reservoir water which contrasts with the solute-poor chemistry of a local cold stream. The contrasting hydrogeology of Kverkfjöll and Askja demonstrate the influence of topography on both the surface expressions and surface chemistry of volcanic hydrothermal systems (VHSs). Notably, however, these differences are expressed mainly in the compositions of the thermal springs, whereas the compositions of high-flux fumarole vapors mainly reflect deeper processes in the system.

S2. Reconstructing the Reservoir Liquid Composition and Temperature

The temperature and composition of the reservoir liquid of Kverkfjöll, i.e., the deep parental hydrothermal fluid prior to phase separation and shallow modifications, was reconstructed from the chemistry of the hot spring waters and fumaroles using techniques outlined below.

S2.1 Reservoir fluid temperatures

To estimate reservoir fluid temperatures, three types of gas geothermometers were applied: Silica-enthalpy mixing model (Fig. S1; Truesdell and Fournier, 1977), noble gas thermometer

(reported previously in Byrne et al. 2021) as well as various gas thermometers (Árnorsson and Gunnlaugsson, 1985, Arnórsson 1998). The silica-enthalpy mixing model yields a reservoir liquid temperature of ~280 °C for Kverkfjöll (Fig. S1). The noble gas T_{Ar-Kr} and T_{Ar-Ne} thermometers yield temperatures of 263 to 332 °C for Kverkfjöll and 337 to 345 °C for Askja (Byrne et al., 2021). The H_2, H_2S, H_2S/H_2, H_2S/Ar and H_2/Ar gas thermometers of Árnorsson et al. (1998), applied for available fumarole compositions for Askja (n = 9) and Kverkfjöll (n = 34; Poreda et al., 1992; Ólafsson et al., 2000; Stefánsson, 2017; Byrne et al., 2021; this study) give a mean reservoir temperature of 290±30 °C for Kverkfjöll and 290±40 °C for Askja. We did not use the gas thermometers based on CO_2 concentrations, as these commonly show excess temperatures in Iceland, likely due to the high CO_2 flux prohibiting attainment chemical equilibrium in the reservoir (Arnórsson, 2000; Byrne et al., 2021)

The general agreement between the major gas, silica-enthalpy and noble gas thermometers is notable, given that they are based on entirely independent underlying assumptions: The major gas thermometers assume *chemical* mineral-fluid equilibrium in the reservoir, whereas the noble gas thermometer is based on the elemental fractionation during the *physical* process of boiling. The high temperature (c. 280°C) estimated for the thermal source fluid of the Hveragil river suggests that mixing of reservoir liquid and cold groundwater likely takes place at depth after minimal amount of boiling. Mixing taking place above the decompression boiling pressure would prevent further boiling during the upflow (c.f. Arnórsson and Barnes, 1983).

S2.3 Reservoir fluid compositions

The linear trends shown by the Hveragil thermal water samples for most major, minor and trace elements vs. temperature (Figs. S1, S2a) show that it represents a rare natural example of a binary mixture of nearly unboiled reservoir liquid and shallow groundwater of local meteoric water origin. Silica-enthalpy mixing thermometer (Truesdell and Fournier, 1977) can thus be applied to yield both a reservoir liquid temperature of ~280 °C as well as a meteoric/reservoir water mixing ratio or mixing proportion for a given sample. Then, the concentration of a conservative element i in the reservoir fluid ($C_{i,res}$) can be calculated using the concentrations i in meteoric water ($C_{i,cold}$; average of three Hveragil cold streams) and the Hveragil sample H-4 ($C_{i,hve}$) with a binary mixing equation

$$C_{i.res} = [C_{i.hve} - C_{i,cold}(1 - f)]/f \qquad (4)$$

The reconstructed reservoir fluid composition of Kverkfjöll is presented in Table 3. A simple mixing model cannot be applied to reconstruct the reservoir fluid composition at Askja samples, because there are no surface outflows of the reservoir or boiled reservoir liquid. Instead, all surface springs at Askja, as well as Lake Öskjuvatn, have a high component of condensed fumarolic vapor, as reflected by their high SO_4 contents (Fig. S2a) and the the poorly defined mixing trajectory in Fig. S1.
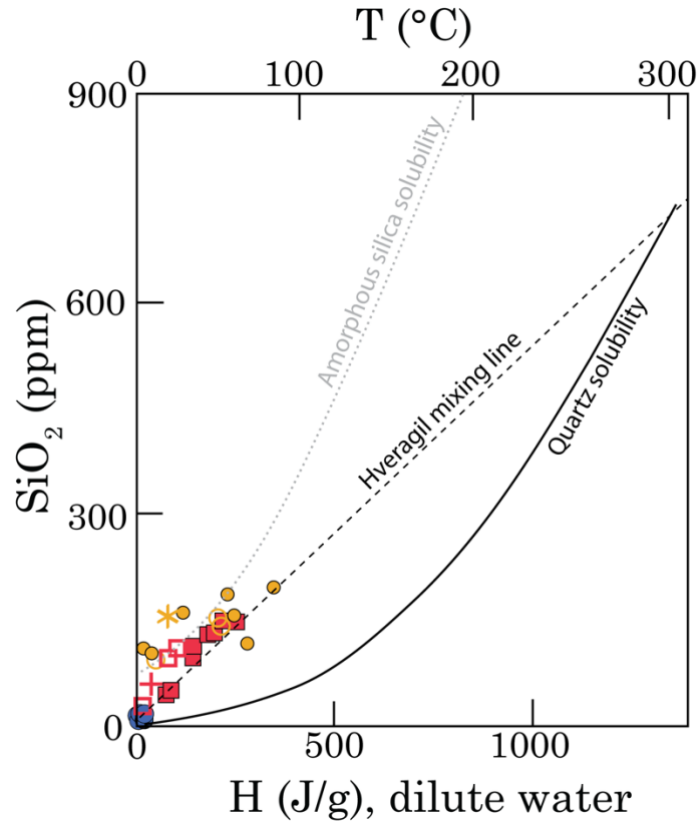
Figure S1: Silica-enthalpy mixing model. The quartz solubility model of Arnórsson et al. (1983) was used together with the silica-enthalpy mixing model of Truesdell and Fournier (1977) to estimate the reservoir fluid composition (section 4.2). Solubility curves for amorphous silica, chalcedony and quartz from Fournier (1977) and Fournier and Potter (1982) are plotted for reference. Symbols as in Fig. 1. Additional Öskjuvatn samples (filled orange circles) from Ólafsson (1980).

.

S2.3 Reservoir fluid composition: fumaroles

The reservoir fluid concentrations of volatile species can be estimated from the fumarole chemistry. We make the assumption that the fumarole vapors form by closed system adiabatic boiling of a dilute, one-phase reservoir liquid. Then, because of conservation of enthalpy, the vapor fraction, x_v, can be calculated by

$$x_v = \frac{h_{liq,res-T} - h_{liq,bp}}{h_{v,bp} - h_{liq,bp}}$$ (5)

where $h_{liq,res}$ is the enthalpy of the dilute reservoir liquid at the estimated reservoir temperature, and $h_{liq,bp}$ and $h_{v,bp}$ are the enthalpies of water liquid and vapor at the sampling temperatures, which can be acquired from standard steam tables. Then, the reservoir liquid concentration of a volatile element i can be calculated by

$$C_{i,res} = x_v \times C_{i,v} + (1 - x_v) \times C_{i,lq} \times B_i$$ (6)

where B_i is a modified distribution coefficient accounting for the dissociation of gas species in the liquid, (Arnórsson and Sigurdsson, 1982). $C_{i,res}$, $C_{i,liq}$ and B_i are solved using the WATCH 2.4 software (Bjarnason, 2010). For average S and CO_2 concentrations of the Kverkfjöll fumaroles, and assuming degassing of ΣS^{2-} and CO_2 from the reservoir liquid between 280°C

to the fumaroles at 100°C using Eqs. (5) and (6), the reservoir ΣS and CO_2 concentrations are estimated at ~200 ppm and 5400 ppm, respectively.

The isotope compositions of the Kverkfjöll reservoir liquid (δD and $\delta^{18}O$-H_2O, $\delta^{13}C$-ΣCO_2, $\Delta^{33}S$-$\delta^{34}S$) were estimated by iteratively finding a starting composition that matches the average fumarole isotope values after taking account adiabatic boiling between 280°C and 100 °C (Fig. 3). The used fractionations factors and calculation details are outlined in Stefánsson et al., 2015, 2016b, 2017). In short, the effects of boiling on the speciation of S and C in the liquid and vapor phases were computed first with WATCH. These were then used together with available equilibrium isotope fractionation factors to calculate $\delta^{13}C$ and $\delta^{34}S$ fractionation during boiling (Table S2). For δD and $\delta^{18}O$-H_2O, the effects of boiling were calculated using Eq. (5) and vapor-liquid fractionation factors for δD and $\delta^{18}O$ from Horita and Wesolowski (1984).

S3 Constraining Water-Rock Interaction

The dissolution of basalt and formation of secondary minerals is modelled using the PHREEQC program (Parkhurst and Appelo, 1999). The solutions are calculated at 300 °C using the composition of the sample KVK-168 (Ranta et al., 2022) with degassed S (300 ppm) and CO_2 (1 ppm) concentrations. The output of the model is used for isotopic modelling of δD-$\delta^{18}O(H_2O)$ (Table S3; Fig. 3a) using a compilation of mineral-water fractionation factors from Kleine et al. (2020).

S4 Sulfur isotopes of sulfate in thermal waters

When the reservoir liquid cools as a result of adiabatic boiling or mixing with cold groundwater, $\Sigma S^{2-}(lq)$ oxidizes to $SO_4(lq)$ (Stefánsson et al., 2015). Similar oxidation may take place when fumarole gases pass a shallow aquifer, which likely occurs at Lake Öskjuvatn at Askja, which is characterized by high SO_4 concentrations (Fig. S2a). In this case, oxidation can be represented by the reaction

$$H_2S(g) + 4H_2O(lq) \leftrightarrow SO_4^{2-}(lq) + 2H^+ + 4H_2 \tag{7}$$
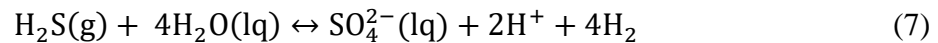
Assuming that oxidation takes place under closed system conditions, S isotope fractionation can be calculated following Ono et al. (2007, 2012):

$$\delta^x S(SO_4^{2-}) = [\delta^x S(H_2S) + 1] \times \frac{1-f^{x\alpha}}{1-f} - 1 \tag{8}$$

where f is the fraction of sulfide remaining, x is 33, 34 or 36 and α is the fractionation factor of S between sulfate and sulfide. Value for $^{34}\alpha$ is estimated using Eq. 11 of Ono et al. (2012), whereas $^{34}\alpha$ is related to $^{33}\alpha$ through

$$^{33}\alpha = {}^{34}\alpha^\theta \tag{9}$$

where θ is the triple fractionation coefficient calculated with Eq. (12) of Ono et al. (2012). The S-$\Delta^{33}S$-$\delta^{34}S$ values of the Öskjuvatn springs are consistent with sulfate being derived from

>90% closed-system oxidation of Askja fumarole H_2S at 200-300 °C (Fig. S3). The $\Delta^{33}S$-$\delta^{34}S$ values of Hveragil and Volga waters can be explained by similar amount of oxidation of the reservoir liquid sulfide, and a minor effect from mixing with a low-S (0.55 ppm) meteoric water component (Fig. 3c).
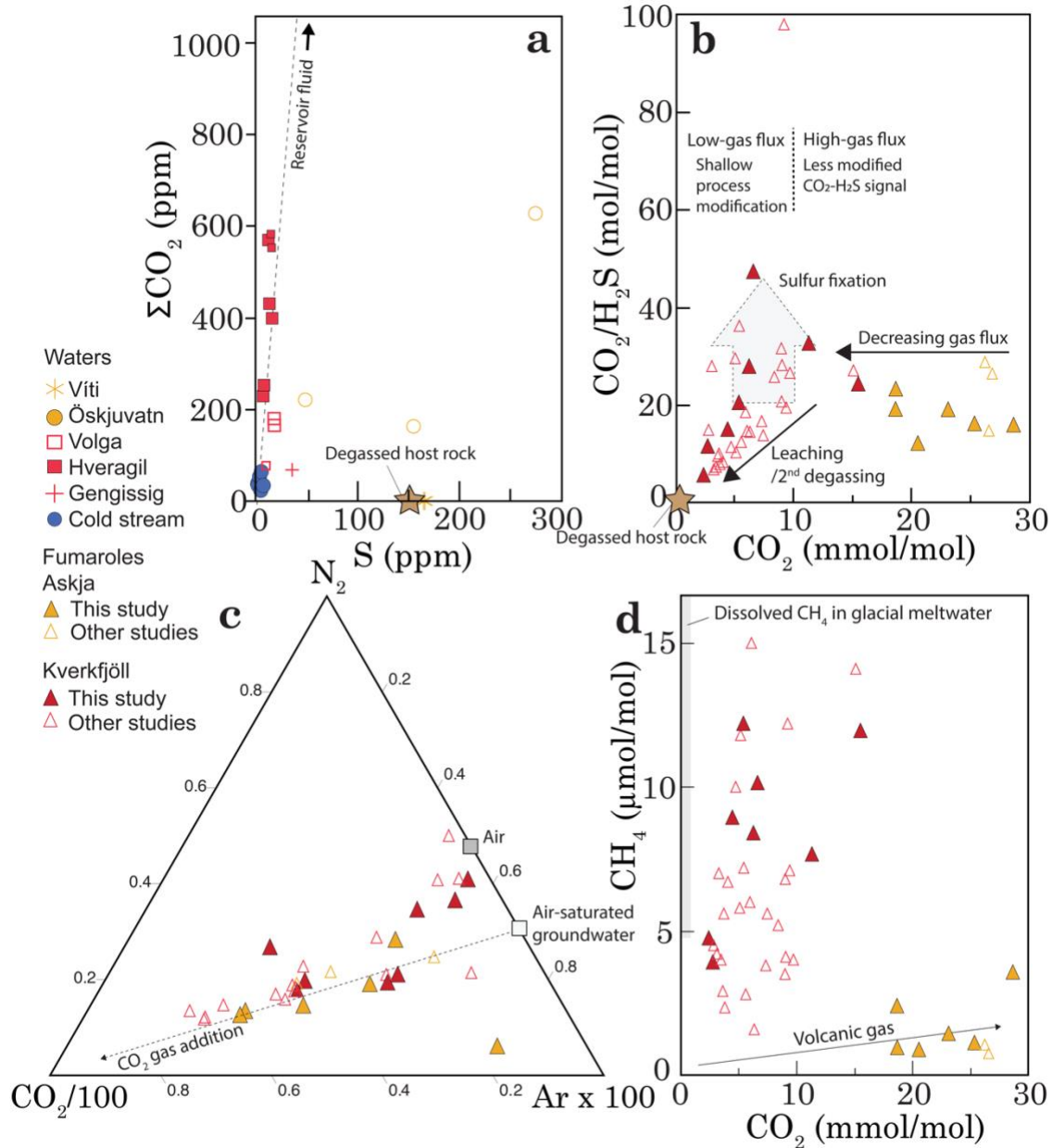

Figure S2. Water and gas chemistry. (a) CO_2 versus. ΣS in thermal and non-thermal waters. (b) CO_2/H_2S versus CO_2 in fumaroles. (c) N_2-CO_2-Ar ternary diagram. Fumarole vapors record N_2/Ar ratios between air and air-saturated groundwater but require external addition of CO_2. (d) CH_4 versus CO_2. The CH_4 concentrations are higher in Kverkfjöll fumaroles. High CH_4 could be derived from glacial meltwater, which can have high CH_4 concentrations (Burns et al., 2018).
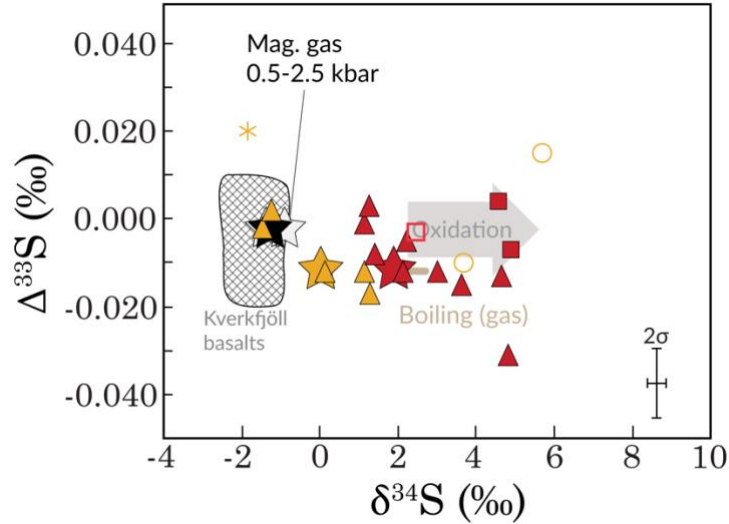
Figure S3. $\Delta^{33}S$ vs $\delta^{34}S$ of H_2S (in fumaroles) and SO_4 (in water samples) from Askja and Kverkfjöll. Symbols as in Fig. 3.

S5 Flux Calculations

S5.1 Eruptive volatile flux potential

Eruptive fluxes (volatiles released from melts during volcanic eruptions) are calculated as

$$F_{erup,i} = f_{erup,i} \times C_{i,.0} \times M_{erup} \tag{10}$$

Where $F_{erup,i}$ (kg/s) is the eruptive flux of volatile i (= H_2O, CO_2, S, Cl), M_{erup} is the eruptive mass flux of basalts (kg/s) and f_i is the fraction of i that is degassed relative to its mass concentration $C_{i,.0}$ in the undegassed melt, i.e.,

$$f_{erup,i} = 1 - C_{erup,i}/C_{i,0} \tag{11}$$

where $C_{erup,i}$ is the concentration of volatile i in the melt after degassing at P = 1 bar.

S5.2 Total intrusive volatile flux potential

We estimate the total intrusive volatile flux by calculating

$$F_{tot,i} = C_{i,.0} \times M_{erup} \times X \tag{12}$$

where X is the intrusion/extrusion production ratio. We assume an X value of 4-8, suggested for Iceland by White et al. (2006). The calculated $F_{tot,i}$ is an estimate for the total transport of mantle volatiles by crust-forming basaltic melts and does not differentiate between volatiles that remain in the crust and volatiles that are degassed into the atmosphere.

S5.3 Intrusive fluxes from decompression degassing

The intrusive volatile fluxes that exsolve from ascending melts via decompression degassing, $F_{intr,i}$, are calculated as

$$F_{intr,i} = f_{intr,i} \times C_{i,0} \times M_{erup} \times X \qquad (13)$$

where $f_{intr,i}$ is the fraction of volatile i that is degassed by decompression degassing, given by

$$f_{intr,i} = 1 - C_{intr,i}/C_{i,0} \qquad (14)$$

The concentration of volatile i remaining in the melt after decompression degassing ($C_{intr,i}$) of an originally volatile-undersaturated melt (with concentration of i $C_{i,0}$) is calculated using the SolEx 1.0 program (Witham et al., 2012)

S5.4 Pre-eruptive volatile concentrations

We model closed and open system decompression degassing to 0.5 and 2.5 kbar using a range of estimated undersaturated H_2O-CO_2-S-Cl concentration of typical tholeiitic melts ($C_{i,0}$) with MgO = 5-8 wt.%. This MgO interval approximately represents the bulk of erupted basalts in Iceland (Hartley and Maclennan, 2018). Composition of the modeled volatile content of the melt is shown in Fig. 9a. For the flux calculations, the undegassed concentrations are estimated at 0.2 to 1 wt.% H_2O, 100-350 ppm Cl and 600-1000 ppm S and 0.1-0.4 wt.% CO_2. For H_2O, Cl and S, these values are based on typical ranges of previously established pre-eruptive concentrations of these volatiles measured in melt inclusions and subglacial glasses (Sigvaldason and Óskarsson, 1976; Nichols et al., 2002; Halldórsson et al., 2016; Bali et al., 2018; Hauri et al., 2018; Miller et al., 2019), which are assumed to represent undersaturated concentrations due to the relatively high solubility of these volatiles at magma storage depths (> ~1 kbar). For CO_2, which is less soluble and because CO_2-undersaturated MIs for high CO_2-melts are unlikely to form at crustal pressures, the higher concentration estimate (4000 ppm) is deemed to be representative based on inferred mantle ratios of C/Ba of 10-35 (equivalent to CO_2/Ba = 37-130; Matthews et al., 2021) and typical Ba concentrations of 10-150 ppm in rift basalts (Ranta et al., 2022). However, because of the complexities related to the mantle C/Ba estimates (Matthews et al., 2021), the upper estimate of the undersaturated melt CO_2 concentrations is the least well constrained of the above values.

S6 Non-magmatic volatile sources

In addition to direct magma degassing, VHSs in Iceland may receive volatiles from the groundwater, atmosphere or crustal rocks. The H_2O—the bulk of the hydrothermal fluids—is almost exclusively of non-magmatic origin (i.e., meteoric or seawater). Fumarolic H_2 is likely derived from H_2O reduction via fluid-rock reactions (Ricci et al., 2022). Noble gases heavier than He as well as N in hydrothermal fluids are mainly of atmospheric origin and derived from air or air-saturated groundwater recharge (Fig. S2c; Füri et al., 2010, Labidi et al., 2020, Byrne et al., 2021). Crustal rocks may contribute to the volatile budget of hydrothermal fluids via fluid-rock interaction. The Icelandic crust comprises mostly subaerially and subglacially erupted basaltic lava flows and intrusions (e.g., Óskarsson et al., 1982). Due to the low melt

solubility of CO_2 and S at low pressures (Fig. 4.4b) and crystallization-driven fluid exsolution following lava or intrusion emplacement (Edmonds and Woods, 2018), both lavas and intrusions tend to be poor in CO_2 (< 10 ppm; Barry et al., 2014) and S (~90 ppmw; average of 9 lava flows; Torssander, 1989). Thus, the igneous crust is likely to be only a minor source of C—supported by the magma gas-like $\delta^{13}C$ signature of hydrothermal source fluids (Fig. 4.3d)—-whereas small amounts of S may be leached from the crust. Crustal sedimentary sources of C or S are almost absent kn the Icelandic crust, although CH_4, which is a minor component in fumarole gases (1-13 μmol/mol), may have a biogenic origin along with other trace hydrocarbons (Fiebig et al., 2020). Basalt-like Cl/B (Stefánsson et al., 2019) and $\delta^{37}Cl$ compositions of Icelandic thermal fluids, as well as excess Cl concentration relative to source waters point to rock dissolution as the main source of Cl and B in Icelandic meteoric water-fed VHSs, whereas higher Cl concentrations measured in coastal VHSs result from seawater input (Stefánsson and Barnes, 2016, Stefánsson et al., 2017, Gunnarsson-Robin et al., 2017).
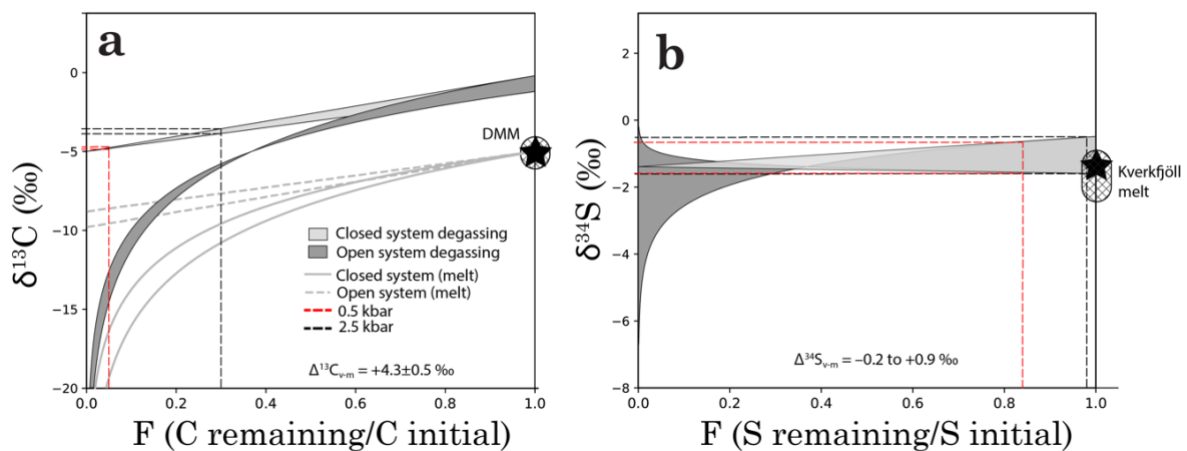

Figure S4. Isotopic composition of magmatic gas. (a) $\delta^{13}C$-CO_2 and (c) $\delta^{34}S$ vs F. The isotopic composition of an exsolved magmatic gas is shown for open- and closed system degassing paths. Black and red dashed lines mark the isotopic composition of the gas at F (fraction of C or S remaining in the melt) and corresponding to closed system degassing of intrusions to 2.5 and 0.5 kbar, respectively. The $\delta^{13}C$-CO_2 values of magmatic gas become progressively lower during degassing of a basaltic melt, whereas $\delta^{34}S$ may become either slightly more positive or negative depending on the melt and gas redox states (Mandeville et al., 2009). However, because only minor degassing of S occurs during melt ascent to 2.5 kbar or even 0.5 kbar, the $\delta^{34}S$ values of both deep and relatively shallow magmatic gases are indistinguishable from the initial melt signatures. By contrast deep degassing may yield gas with up to 4.8 ‰ more positive $\delta^{13}C$-CO_2 values relative to initial melt. Crystallization-driven degassing of intrusions would follow the closed- or open system degassing paths toward lower F. Initial melt $\delta^{13}C$ and $\delta^{34}S$ signatures as in Fig. 5.

Supplementary References

Arnórsson, S., & Barnes, I. (1983). The nature of carbon dioxide waters in Snaefellsnes, western Iceland. *Geothermics*, *12*(2-3), 171-176.

Arnórsson, S., Gunnlaugsson, E., and Svavarsson, H. (1983). The chemistry of geothermal waters in Iceland. III, Chemical geothermometry in geothermal investigations. *Geochimica et Cosmochimica Acta*, *47*(3), 567-577.

Arnórsson, S., Sigurdsson, S., & Svavarsson, H. (1982). The chemistry of geothermal waters in Iceland. I. Calculation of aqueous speciation from 0 to 370 C. *Geochimica et Cosmochimica Acta*, *46*(9), 1513-1532.

Arnórsson, S. (ed.) (2000), Isotopic and chemical techniques in geothermal exploration, development and use. Sampling methods, data handling, interpretation. International Atomic Energy Agency, Vienna, 267-308.

Burns, R., Wynn, P. M., Barker, P., McNamara, N., Oakley, S., Ostle, N., Stott, A.W., Tuffen, H., Zhou, Z., Tweed, F.S., Chesler, A., & Stuart, M. (2018). Direct isotopic evidence of biogenic methane production and efflux from beneath a temperate glacier. *Scientific reports*, *8*(1), 1-8.

Fournier, R.O. (1977) Chemical geothermometers and mixing models for geothermal systems, *Geothermics*, *5*(1-4), 41-50,

Fournier, R.O., &Potter, R.W. (1982) Revised and expanded silica (quartz) geothermometer. *Geothermal Resources Council Bulletin*, *11*(10).

Hartley, M., & Maclennan, J. (2018). Magmatic densities control erupted volumes in Icelandic volcanic systems. *Frontiers in Earth Science*, *6*, 29.

Hauri, E. H., Maclennan, J., McKenzie, D., Gronvold, K., Oskarsson, N., & Shimizu, N. (2018). CO_2 content beneath northern Iceland and the variability of mantle carbon. *Geology*, *46*(1), 55-58.

Heřmanská, M., Stefánsson, A., & Scott, S. (2019). Supercritical fluids around magmatic intrusions: IDDP-1 at Krafla, Iceland. *Geothermics*, *78*, 101-110.

Miller, W. G., Maclennan, J., Shorttle, O., Gaetani, G. A., Le Roux, V., & Klein, F. (2019). Estimating the carbon content of the deep mantle with Icelandic melt inclusions. *Earth and Planetary Science Letters*, *523*, 115699.

Stefánsson, A., Arnórsson, S., Sveinbjörnsdóttir, Á. E., Heinemaier, J., & Kristmannsdóttir, H. (2019). Isotope (δD, δ^{18}O, ^{3}H, δ^{13}C, ^{14}C) and chemical (B, Cl) Constrains on water origin, mixing, water-rock interaction and age of low-temperature geothermal water. *Applied Geochemistry*, *108*, 104380.